Numerical Simulation of Shock Response of Disk-Suspension-Slider Air Bearing Systems in Hard Disk Drives

Q. H. Zeng and D. B. Bogy
Computer Mechanics Laboratory
Department of Mechanical Engineering
University of California
Berkeley, CA 94720

Abstract

As non-traditional applications of hard disk drives emerge, their mechanical robustness during the operating state is of greater concern. A procedure for simulating the shock responses of a disk-suspension-slider air bearing system is proposed in this paper. A finite element model of the system is developed and modified, and it is used to obtain the dynamic normal load and moments applied to the air bearing slider. The dynamic load and moments are then used as input data for the air bearing dynamic simulator to calculate the dynamic flying attitudes. We obtain not only the responses of the structural components, but also the responses of the air bearing slider. The procedure is convenient for practical application, because it separates the work into two essentially uncoupled steps. It is used to simulate the shock response of a drive, which reveals a beating phenomenon that can be eliminated by changing the arm design. The system modeled is linear before the dimple separates due to a strong shock, and then it is non-linear. The air bearing has different responses for upward and downward shocks. Slider-asperity contacts occur when a strong shock is applied.

1 Introduction

The interest in the effects of shock on hard disk drives has come into currency due to the increasingly hostile environments encountered in the usage of the portable computer. As non-traditional applications of hard disk drives emerge, their mechanical robustness under shock and other mechanical disturbances during different states is of greater concern. A typical example is a PC with a disk drive installed on high speed boats. Read/write operation of the drive is frequently aborted because of the shocks caused by wave actions. Normal drives cannot properly function in this kind of environment. The main effects of shock are malfunctions during the operating state, damage during initial assembly, testing, installation into the computer chassis, and all unfavorable situations caused by the final users. There are essentially three approaches for dealing with the shock problems. The first is to design a suitable isolation installation for the disk drives. The second is to design a robust servo control mechanism to prevent read/write error during the shock. The third is to design a robust mechanical system and slider/disk interface. We focus on the latter approach. There have been several experimental and simulation studies [1-5] on shock response of the mechanical system and its effects on the head/disk interface. However, most of the published works are limited to the non-operating state of the drives, and/or to the component level. As the flying height (FH) continues to decrease and more and stronger disturbances during the operating state are encountered, a better understanding of the effects of the disturbances on the slider/disk interface is required.

Two published papers [6,7] considered shock simulation of disk drives in the operating state. They used quite different approaches. Jiang et al. [6] focused on the rotating disk in their paper. The suspension and slider were modeled as one spring and one mass, and the

air bearing was modeled as another spring. The shock was specified at the end of the suspension and on the disk hub. The solution was obtained by using the multi-modal expansion approximation, applying the Galerkin method to the resulting equations, and using the Newmark β method to solve the final equations. The air bearing responses, i.e., the dynamic FH, was obtained from the deformation of the spring that models the air bearing. Their method is expected to model the disk response very well. However, it cannot provide good insight for the response of the arm-suspension and the air bearing. Harrison and Mundt [7], on the other hand, focused on the air bearing. The suspension and slider were modeled as a lumped multiple DOF spring-mass system. The air bearing was modeled by the usual Reynolds equation, and it was solved by a numerical method. They measured the disk's response at the point under the slider and the arm's response at the end of the arm. Then they used this measured data as input into the air bearing simulation code, and they obtained the dynamic FH. It is inconvenient to apply their method because it requires the measurement data for each case of interest. Furthermore, they didn't describe how to obtain the lumped spring-mass model of the arm-suspension, and they didn't show the effect of this simplification on the results. Therefore, more research is required for shock simulation of the disk drives and slider air bearings during the operating state.

In this paper we propose a procedure for simulating the shock response of a disk-suspension-slider air bearing system. A finite element model of the disk and suspension system is developed then modified and used to obtain the dynamic normal load and moments applied to the slider air bearing. These are then used as input data for an air bearing dynamic simulator to calculate the dynamic flying attitudes. The procedure is applied to simulate the shock response of a disk drive. The results show that the procedure

is convenient for practical application, because it separates the work into two essentially uncoupled steps. We obtain not only the responses of the structural components, but also the responses of the slider air bearings.

2 A Simulation Procedure

2.1 Theoretical Considerations and Assumptions. To better understand shock effects and improve the shock resistance of disk drives, we need to know the shock responses of both the structural components and the slider air bearings. Therefore, we consider both of these, and apply completed finite element (FE) models of the components in the simulation. There are many different cases in the operating state. We consider only the most severe case of the slider located at the outer radius of the disk, and the shock applied in the direction perpendicular to the disk. We consider only negative pressure sliders of the type used in almost all current drives. The sliders have very stiff air bearings [8], and may experience a negative normal load without lift-off from the disk [9].

We assume there is no significant difference in the shock responses of the disk during the operating and non-operating states when the shock is applied axially to the hub (Assumption 1). This assumption is only reasonable if the disk response is axisymmetric. The excitation of the shock is symmetric about the rotation axis of the disk. It is well known that a rotating disk has three types of modes. The first type is the symmetric modes with nodal circles (m, 0), which have frequencies that only slightly increase with the rotating speed. Their frequencies and mode shapes are very similar in the operating and non-operating states. The second is the asymmetric modes with nodal diameters (0, n), each of which splits into two modes in the operating state. They have no response to

symmetric excitations. The third is the coupled asymmetric modes (m, n) (m>0, n>0), which are higher frequency modes, and their responses are much smaller than the responses from the low frequency modes for ordinary shocks (e.g., 2 ms half sinusoidal acceleration). Although the slider's load on the disk is not axisymmetric, we will show in a FE analysis that its contribution to the disk response is negligible. Therefore, the disk responses to a symmetric shock are expected to be mainly from the axisymmetric modes, and they are similar in the operating and non-operating states. Hence, it is expected that this assumption will not cause a significant error in the simulation results, but it limits the application range of the procedure to axial shock.

We also assume that changes of the air bearing stiffness have no significant effects on the shock responses of the structural components (Assumption 2). That is because the stiffness of the air bearings is much greater than those of the structural components. This assumption can be easily verified in the simulation.

2.2 Simulation Procedure. Because of Assumption 2, we can divide the simulation procedure into two main steps. The first step is the calculation of the shock responses of the structural components. The second is the calculation of the dynamic attitudes of the air bearing slider. We can outline the procedure as follows.

I. Create a FE model of the "drive", including at least a disk, an actuator arm, and a suspension.

   a) Create FE models of each component, and verify them by modal experiments. Verification of the FE models at the component level is very important for obtaining

a good system FE model. Especially, the FE models of the disk in both the free and clamped states and the suspension in its free state (not loaded on the disk) should be verified by modal experiments.

b) Integrate the component models into a system FE model, and verify it in the non-operating and operating states by experiments. We mainly compared the calculated modal frequencies with the measured frequencies.

II. Design the air bearing sliders and evaluate the stiffness of the air bearings

a) Design the slider's air bearing surface (ABS).

b) Obtain its stiffness matrix by using the parameter identification method [8] in the steady flying state.

III. Modify the FE model and calculate the shock responses

a) Add contact elements to model the dimple and the limiters if there are limiters in the suspension.

b) Use the stiffness matrix to model the air bearings in the FE model of the drive.

c) Specify the time history of the displacements at the end of the arm and at the hub of the disk to simulate a shock.

d) Calculate the transient responses of the structures, and obtain the force and moments applied to the slider air bearing – dynamic normal load and moments.

IV. Simulate the dynamic flying attitudes of the slider

a) Interpolate the load and use it as input to the CML Air Bearing Dynamic Simulator [10]. Usually, the time step needed in the calculation of the shock responses of the structures is much larger than the one used in the air bearing dynamic simulation, so an interpolation of the dynamic normal load and moments is required. The CML Air Bearing Dynamic Simulator was modified for the shock simulation.

b) Calculate the time histories of the slider attitudes.

3 Case Study

3.1 FE Model and Modal Parameters of a Drive. In our previous paper [11], a FE model of a disk drive with two disks was created by using the ANSYS code, and the model was verified by experiments. The FE model used here, shown in Fig. 1, includes one disk, one actuator arm and one suspension. There are a total of 16020 degrees of freedom (DOF). The inner radius (24.905 mm) of the disk and the inner radius at the pivot end of the arm are designated as a base. The base was constrained to have zero displacement in the six DOFs in the modal analysis. The frequencies of the first six modes are shown in Table 1, and the mode shapes of two of these modes are shown in Fig. 2. This is a linear FE model. After it was verified by experiments, the dimple was modeled with a contact element (CONTAC49) for the shock simulation.

3.2 The Slider Used in the Simulation and Its Properties. The Nutcracker nano slider, as shown in Fig. 3, was used in the simulation. The slider has a calculated FH of 28.18 nm at the outer radius (44 mm, skew -17.39o) of the disk rotating at the 5400 RPM. By using the parameter identification method, we obtained the stiffness matrix of the slider air bearing as

$$K_{air} = \begin{bmatrix} 1.76E+6 & -8.55E+2 & -8.45E+0 \\ -8.55E+2 & 9.67E-1 & 1.04E-2 \\ -8.45E+0 & 1.04E-2 & 3.83E-1 \end{bmatrix}, \text{(N, m, rad)}$$

This matrix was used in the FE model to represent the air bearing during the first part of the shock analysis.

3.3 Shock Responses of the Structures. A 2 ms, 63g half-sinusoidal acceleration shock was applied in the simulation at the base in the Z direction. The displacement of the shock, as shown in Fig. 4, was obtained by using a numerical integration. This displacement history was then specified at the base in the Z direction, while the other five DOFs were fixed. The time step was 50 μs, and the damping ratios used were about 2% for the modes with frequencies about 600 Hz. The Full Transient Dynamic Analysis of the ANNSYS code was applied in the calculation. That means the results are more accurate than those obtained by the Reduced or Modal Superposition methods, but the calculation is very time consuming. The histories of the calculated responses of the arm and the disk relative to the base are shown in Fig. 5. It is seen that the maximum relative displacement of the arm and disk is about 0.1 mm. Figure 6 shows the deformation shapes of the system at different times. It is observed that the contours are exactly circular on the disk, even though Fig. 2 shows the possibility of non-axisymmetric modes. This means that the non-axisymmetric contributions to the shock response are negligible, and therefore the disk responses are from axisymmetric modes that experience little change in the operating state. This means that Assumption 1 is reasonable.

The histories of the force and moments applied to the air bearing were also calculated, and they are shown in Fig. 7. It is seen that the normal load rapidly increases from 3.5 gram to about 6.0 gram, and then oscillates and damps out. However, the trend of the pitch and roll moments are much more complicated. They show a beating phenomenon that results in large pitch and roll oscillations requiring a much longer time to damp out. This is not a good feature for drive performance. Checking the modal frequencies shown in Table 1, one can see that the modal frequency of the 1st bending mode of the arm-suspension is

close to that for the disk (0,0) mode. These two modes generate the beating. The easiest way to avoid the beating phenomenon is to increase the arm's frequencies by modifying the arm design, i.e., by changing its geometry and/or material. Just for demonstration, we doubled the Young's modulus of the original arm, and designated it as a modified design. The frequency of the first beading mode of the modified design increases from 590 Hz to 823 Hz, as shown in Table 1. Figure 8 shows the shock response of the arm and the disk, and the dynamic normal load and moments for the modified design. Comparing Fig. 8 with Figs. 5 and 7, one can see that the oscillations in the modified design damp out much faster than they do in the original design. Therefore, the frequency assignment of the drive significantly affects its shock resistance.

3.4 Shock Responses of the Air Bearing Slider. The dynamic normal load and moments that are shown in Fig. 7 were used as input data to the CML Air Bearing Dynamic Simulator, and the slider's flying attitudes were obtained, as shown in Fig. 9. The Greenwood-Williamson model was used to simulate the asperity contact. A 1 ms time step and 5 nm glide height were specified in the simulation. Figure 9 indicates that the minimum clearance between the slider and the disk is about 2.5 nm. That means there is asperity contact between the slider and the disk when the shock is applied. The maximum FH variation is about 25 nm. The slider has a strong oscillation that takes a relatively long time to damp out because of the beating. Figure 10 shows that the oscillation quickly damps out when the modified arm is used.

3.5 Effects of the Air Bearing Stiffness on the Structural Responses and Slider's Attitudes. Figure 11 shows the effects of the air bearing stiffness on the shock responses.

In order to investigate a wide range of stiffness, we specified stiffness matrices 5 times and 0.2 times the original value. Then we calculated the shock responses of the structures and the slider air bearing. From Fig. 11, it is observed that the dynamic normal loads for all three cases are almost exactly the same. The pitch moments are obviously different, but overall the moments are very small. Therefore, the responses of the slider are quite similar for the three cases as shown also in Fig. 10. These results indicate that the stiffness matrix of the air bearing used in the FE model has no significant effect on the structural response or the slider's attitudes over a wide range of stiffness changes. That means Assumption 2 will not result in a large error. The error will be related to the stiffness differences between the air bearing and the suspension, especially the suspension gimble. The larger these differences are, the smaller is the error. A large stiffness difference is one of the suspension design requirements.

3.6 Comparison of Different Shock Amplitudes. The shock responses were simulated for upward and downward shocks at different shock amplitudes. The results are summarized in Figs. 12-14. It is observed that the maximum normal load changes have a linear relationship with the shock amplitudes from about –100 g to 150 g. However, the changes are not linear when the dimple separates due to the stronger shocks. This is to be expected because the system is linear before the dimple separates, but it is non-linear when there is dimple separation. This result is different from that shown in Fig. 3 in [7]. Peak-to-peak FH variations and minimum clearances with respect to different shock amplitudes are also shown in Fig. 12. The slider-asperity contacts occur when the minimum clearance is less than the glide height (5 nm). The downward shocks result in larger FH variations than the upward shocks. That is because the FH increases greatly due to the normal load

decrease during the period of the applied shocks. However, the upward shocks result in more severe slider/disk contacts than the same level downward shocks because the larger normal loads appear during the period of the upward applied shocks.

4 Conclusion

A procedure for simulating the shock responses of disk-suspension- slider air bearing systems is proposed. We obtain not only the responses of the structural components, but also the responses of slider air bearings. The FE model of the system was developed and modified for the shock simulation, and then it was used to obtain the dynamic normal load and moments applied to the air bearing. The dynamic load and moments were then used as input data for the CML Air Bearing Dynamic Simulator to calculate the dynamic flying attitudes. The procedure is convenient for practical application, because it separates the work into two essentially uncoupled steps. There are two main assumptions in the procedure. Simulation results show that they are justified and will not result in large error, but the procedure can only be applied to shock in the direction perpendicular to the disk.

The procedure was applied to simulate shock responses of a drive. A beating phenomenon was found, and it was shown that it could be eliminated by changing the arm design. The system is linear before the dimple separates due to a strong shock. The air bearing has different responses for upward and downward shocks. Slider-asperity contacts occur when a strong shock is applied.

Acknowledgments

This study is supported by the Computer Mechanics Laboratory at the University of California at Berkeley.

References

[1] Kumar, S., Khanna, V., and Sri-Jayantha, M., 1994, "A study of the Head Disk Interface Shock Failure," The 6th MMM-Intermag Conference paper.

[2] Kouhei, T., Yamada, T., Keroba, Y., and Aruga, K., 1995, "A Study of Head-Disk Interface Shock Resistance," *IEEE Trans. of Magnetics*, Vol. 31, No. 6, pp. 3006-3008.

[3] Ishimaru, N., 1996, "Experimental Studies of a Head/Disk Interface Subjected to Impulse Excitation During Non-operation," *ASME Journal of Tribology*, Vol. 118, pp. 807-812.

[4] Allen, A. M. and Bogy, D. B., 1996, "Effects of Shock on the Head-Disk Interface," *IEEE Trans. of Magnetics*, Vol. 32, No. 5, pp. 3717-3719.

[5] Edwards, J. R., 1999, "Finite Element Analysis of the Shock Response and Head Slap Behavior of a Hard Disk Drive," *IEEE Trans. of Magnetics*, Vol. 35, No. 2, pp. 863-867.

[6] Jiang, Z. W., Takashima, K., and Chonan, S., 1995, “Shock-Proof Design of Head Disk Assembly Subjected to Impulsive Excitation,” *JSME International Journal*, Series C, Vol. 38, No. 3, pp. 411-419.

[7] Harrison, J. C. and Mundt, M. D., 2000, “Flying Height Response to Mechanical Shock During Operation of a Magnetic Hard Disk Drive,” *ASME Journal of Tribology*, Vol. 122, No. 1, pp. 260-263.

[8] Zeng, Q. H., and Bogy, D. B., 1999a, “Stiffness and Damping Evaluation of Air Bearing Sliders and New Designs with High Damping”, *ASME Journal of Tribology*, Vol 121, pp. 341-347.

[9] Zeng, Q. H., Chapin, M., and Bogy, D. B., 1999b, “Dynamics of the Unload Process for Negative Pressure Sliders,” *IEEE Tran. of Magnetics*, Vol. 35(2), pp. 916-920.

[10] Chen, L. S, and Bogy, D. B., 1998, “Air Bearing Dynamic Simulator User Manual V4.21,” Technical Report No. 98-004, Computer Mechanics Laboratory, Department of Mechanical Engineering, University of California, Berkeley.

[11] Zeng, Q. H., and Bogy, D. B., 1999c, “Dynamic Experiment and Analysis of a Hard Disk Drive,” *J. of Vibration and Control*, Vol. 5 (2), pp. 535-557.

Table 1 Modal frequencies of the drive

Mode shape	Original Design	Modified Design
Arm-Susp1st Bend	**714.80**	**822.71**
Disk (1,0)	604.15	602.86
Disk (1,0)	604.82	604.16
Disk (0,0)	**612.86**	**612.33**
Disk (2,1)	713.53	713.09
Disk (2,1)	714.80	714.79

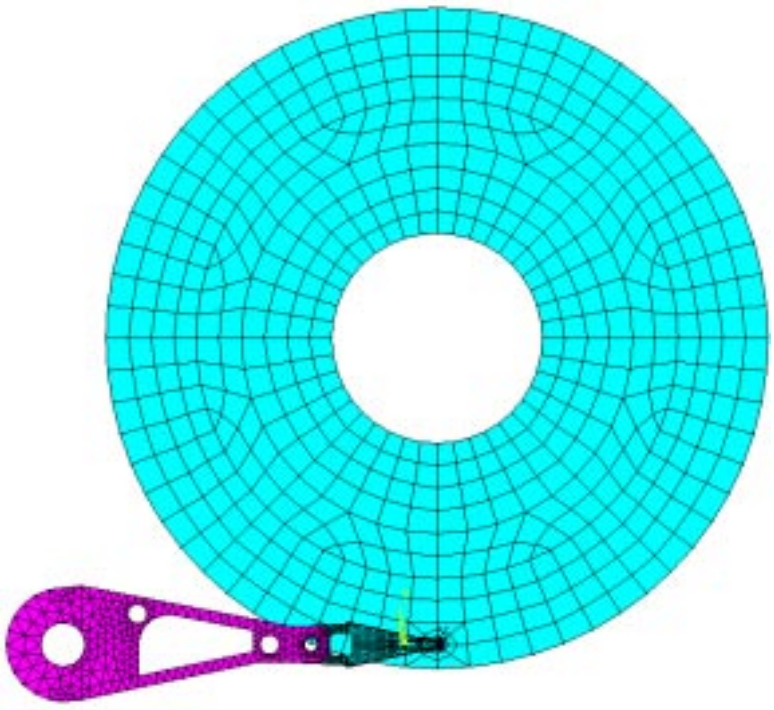

Fig. 1 A FE model of a disk drive

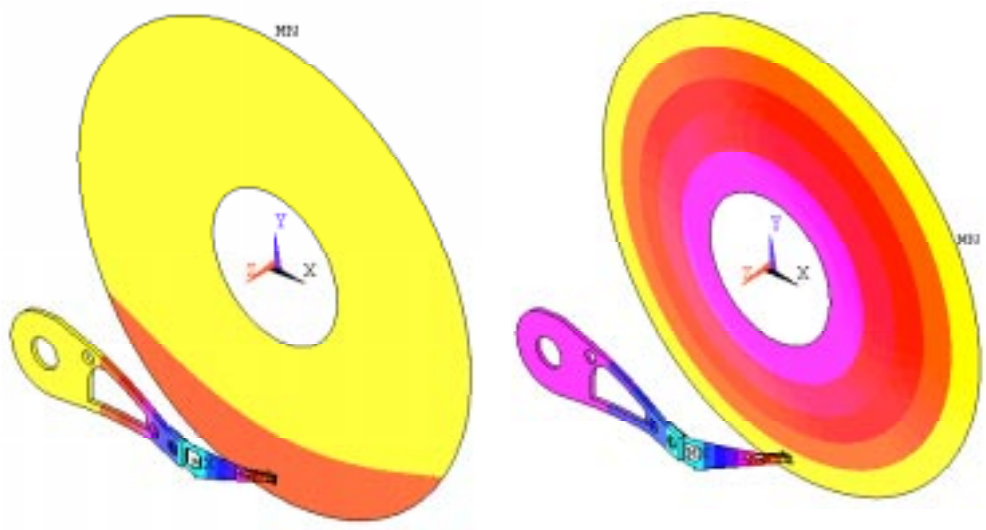

a) 1st Bending of Arm-suspension

b) Disk (0,0) coupled with the 1st bending of the Arm-suspension

Fig. 2 Mode shapes of the drive

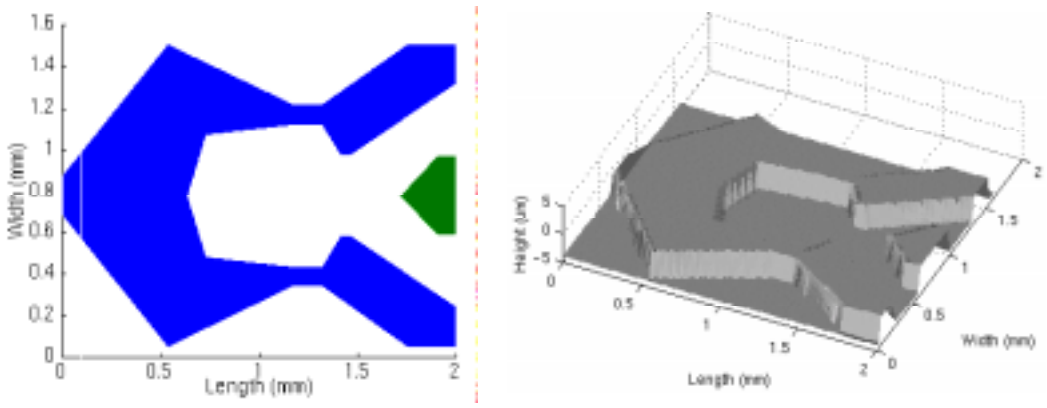

Fig. 3 A slider used in the simulation

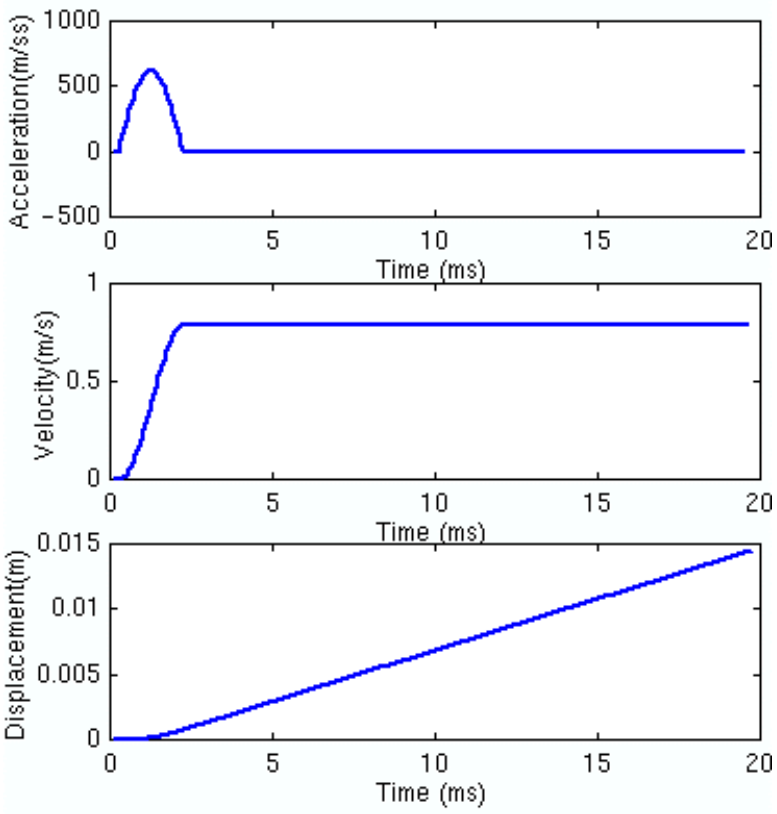

Fig. 4 The shock applied at the base (the end of the arm and the clamp of the disk).

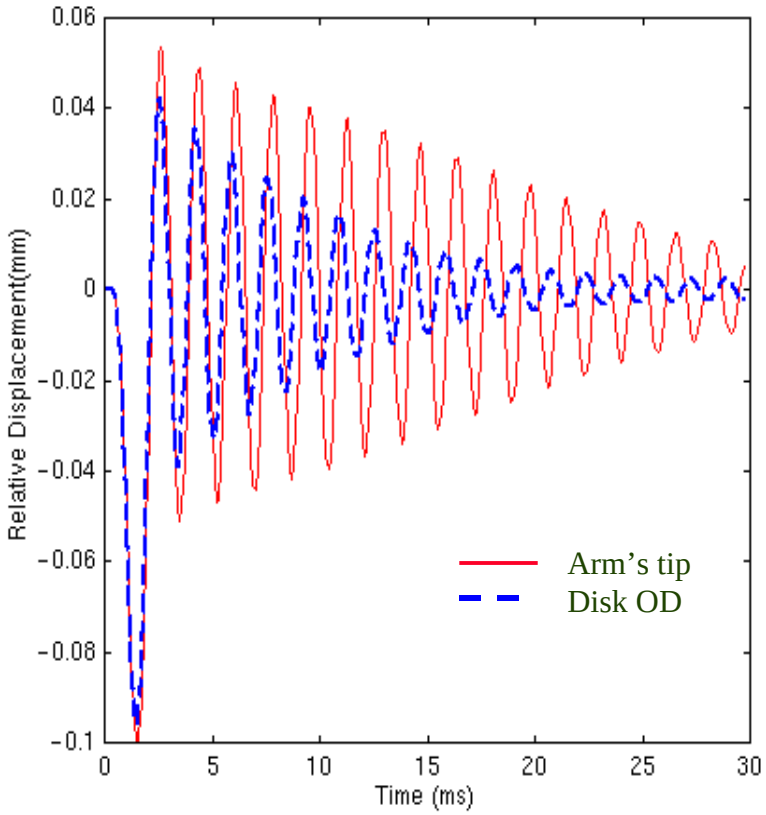

Fig. 5 The calculated responses of the arm and the disk relative to the base

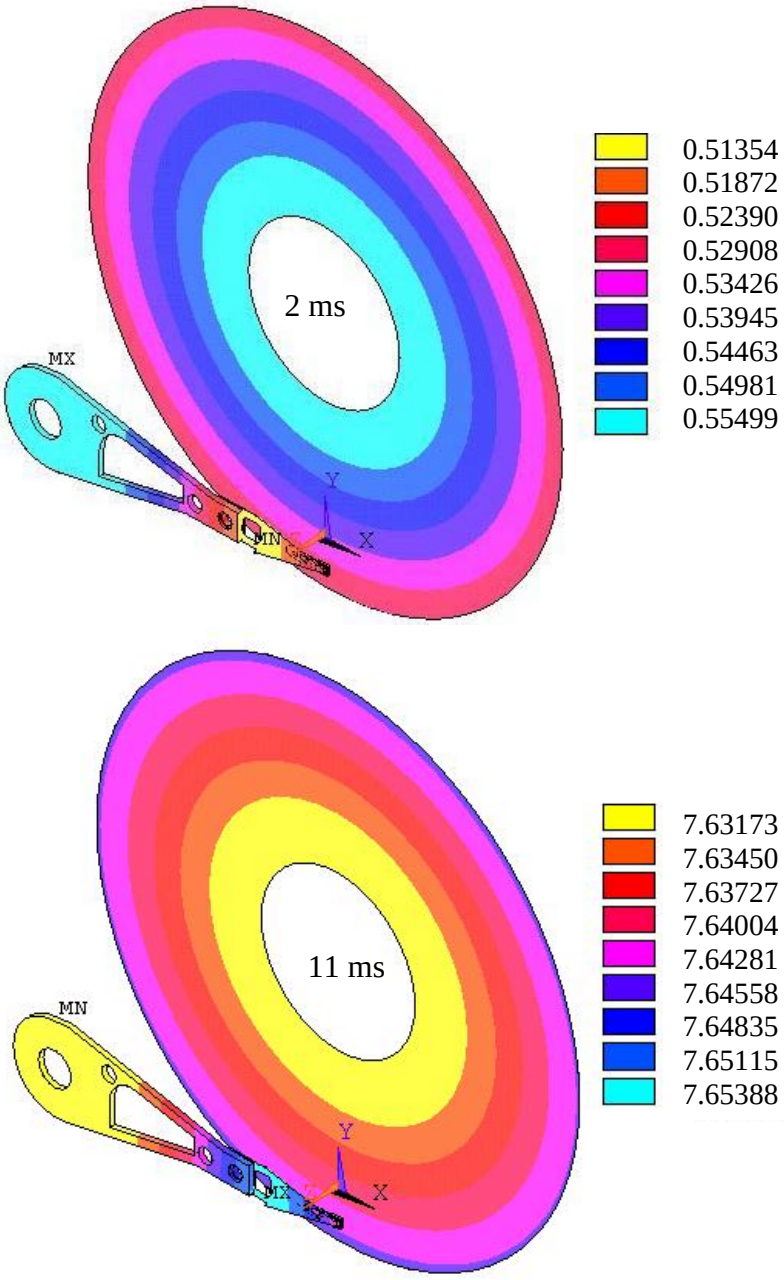

Fig. 6 Shock responses at different times - Contour plot of the absolute displacement (mm)

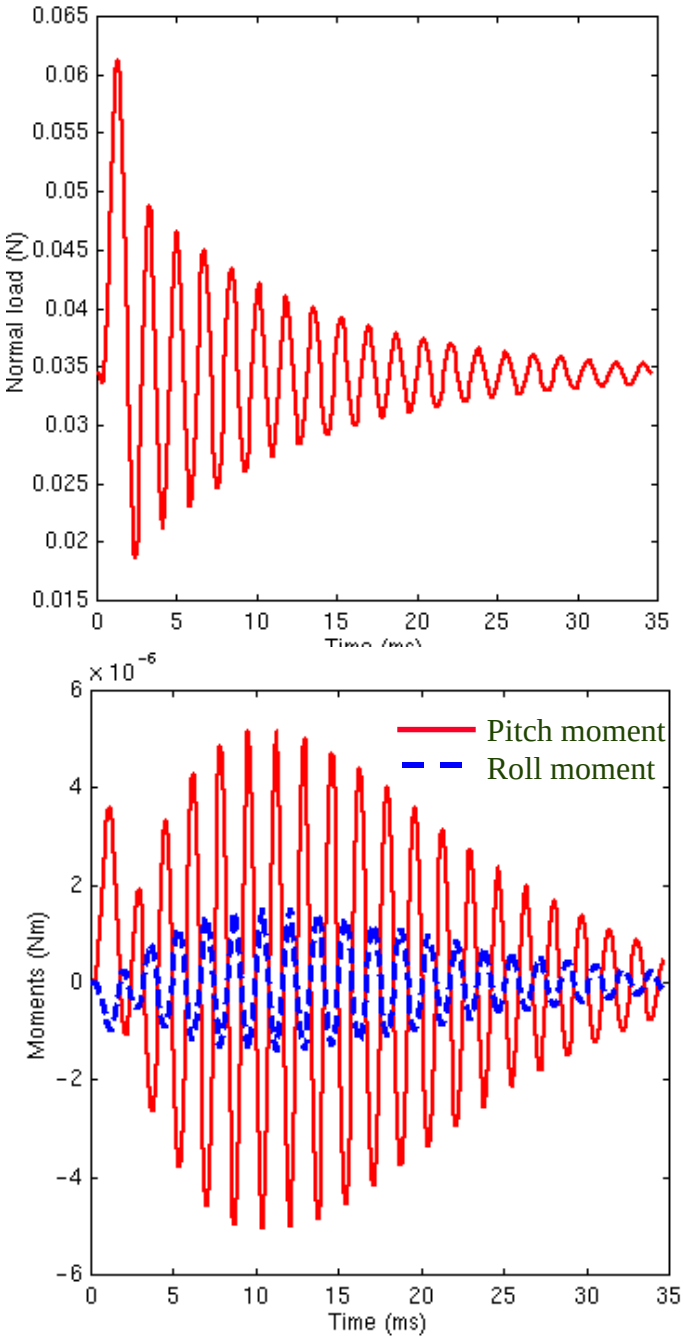

Fig. 7 Calculated dynamic normal load and moments applied to the air bearing

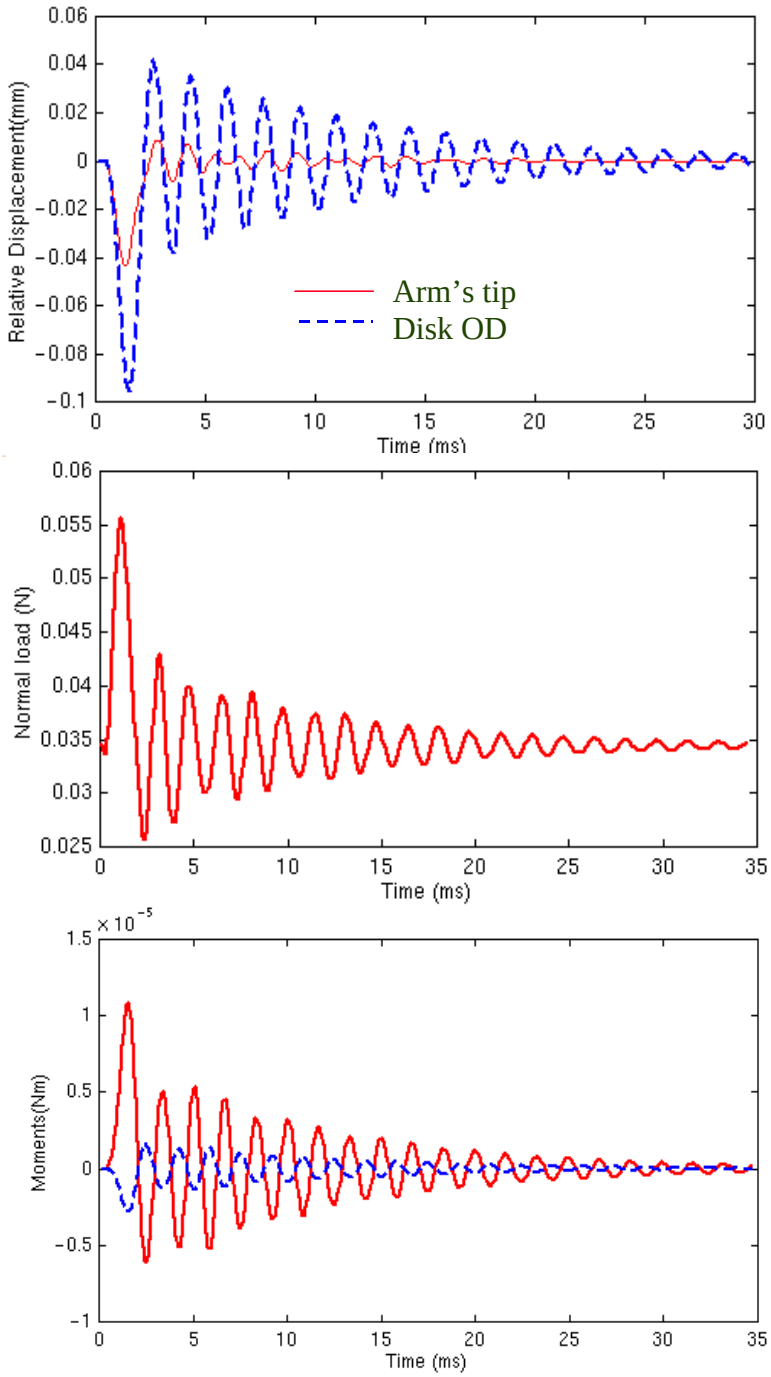

Fig. 8 Shock responses of the drive with the modified arm

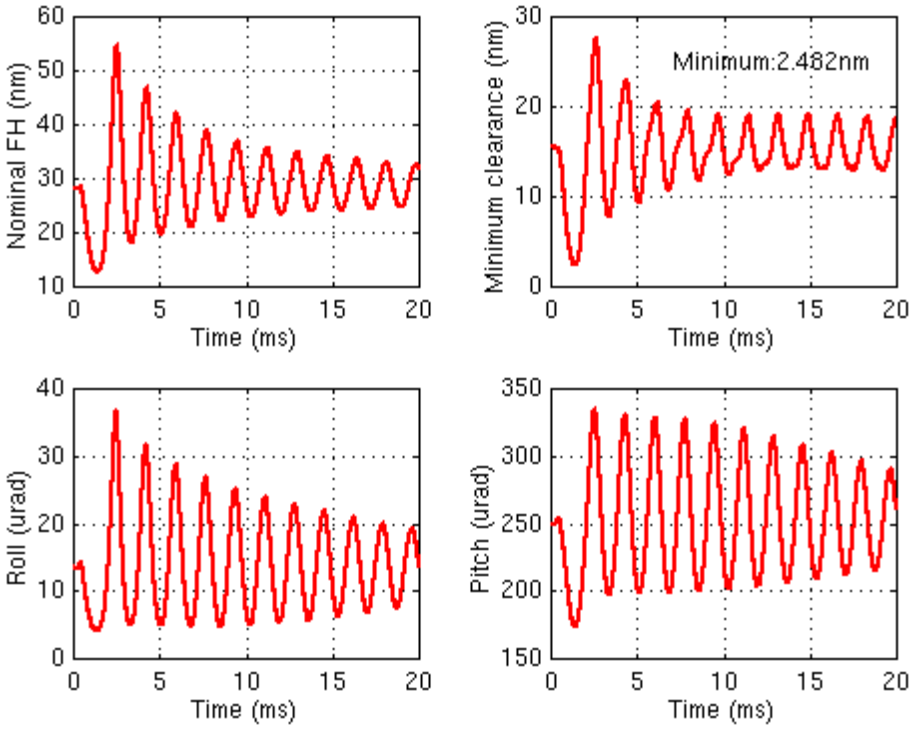

Fig. 9 Shock response of the slider

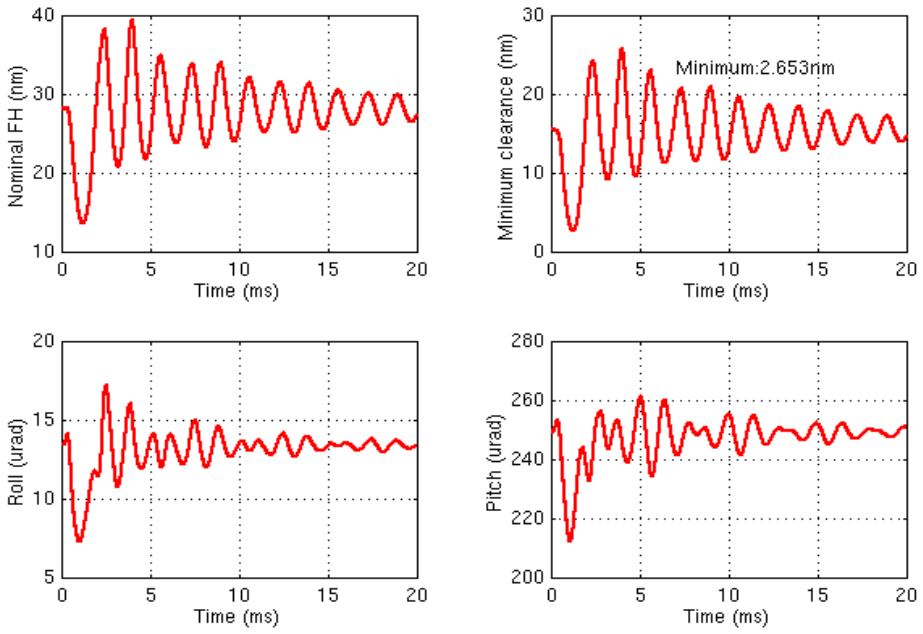

Fig. 10 Shock response of the slider with the modified arm

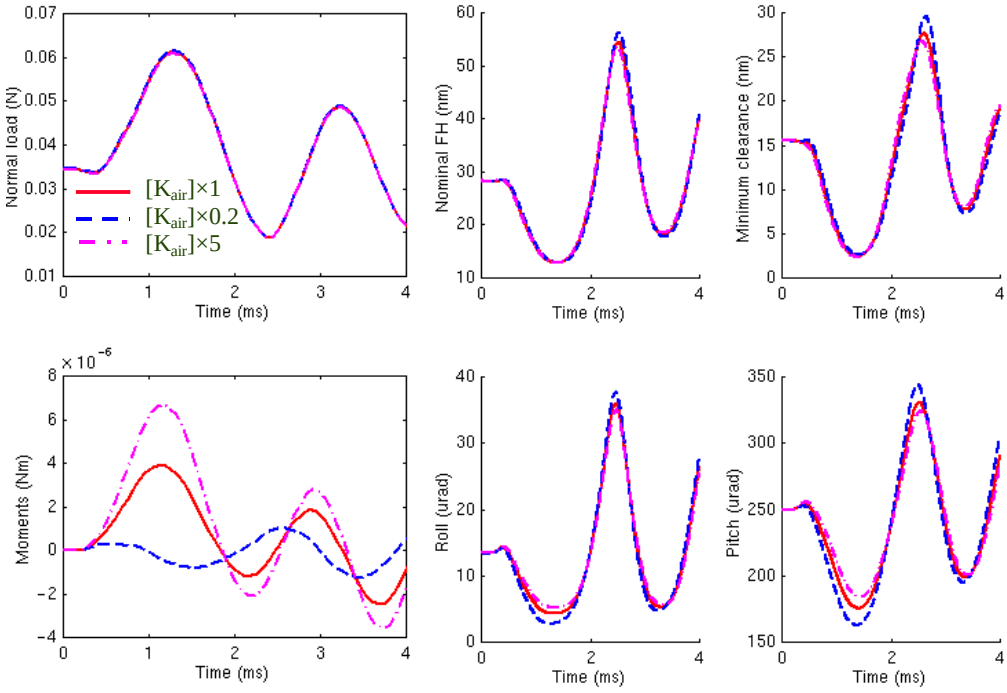

Fig. 11 Effects of the air bearing stiffness on the normal load, moments and slider's attitudes

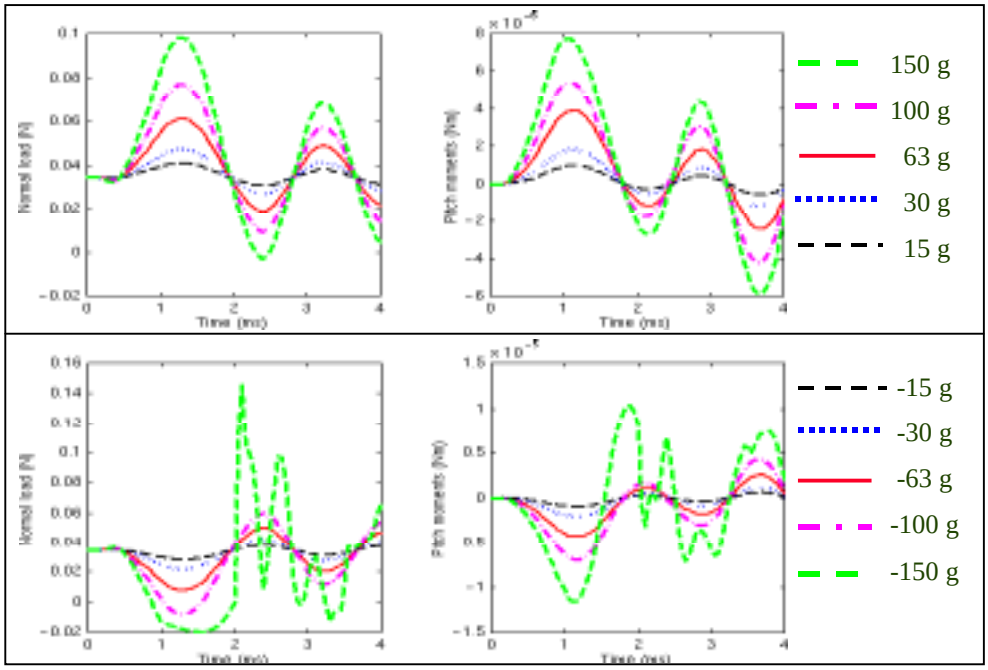

Fig. 12 Comparison of different shock amplitudes - dynamic normal load and moments

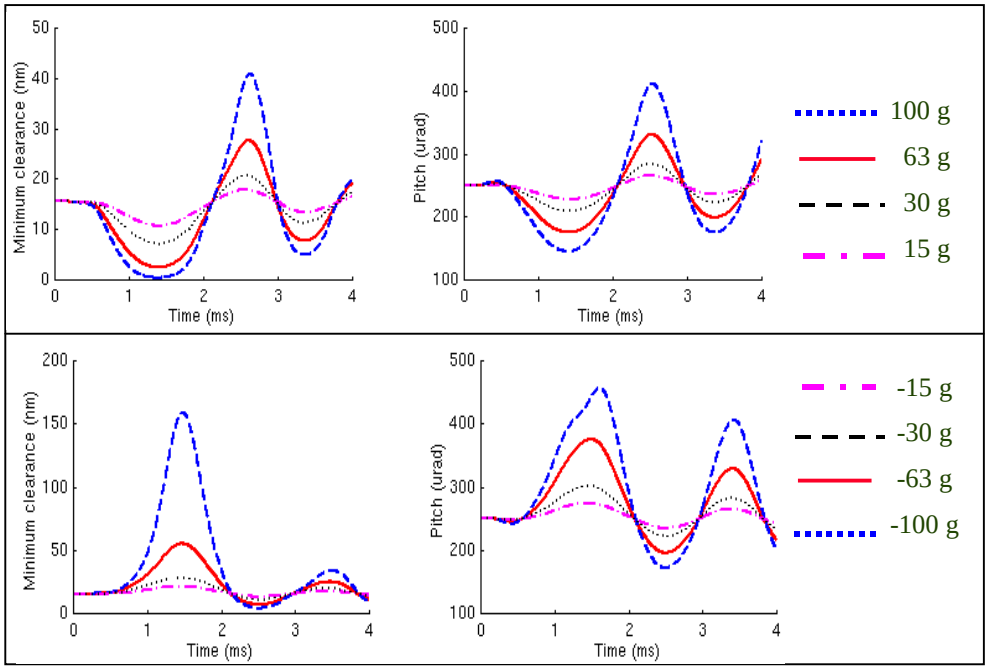

Fig. 13 Comparison of different shock amplitudes - slider's attitudes

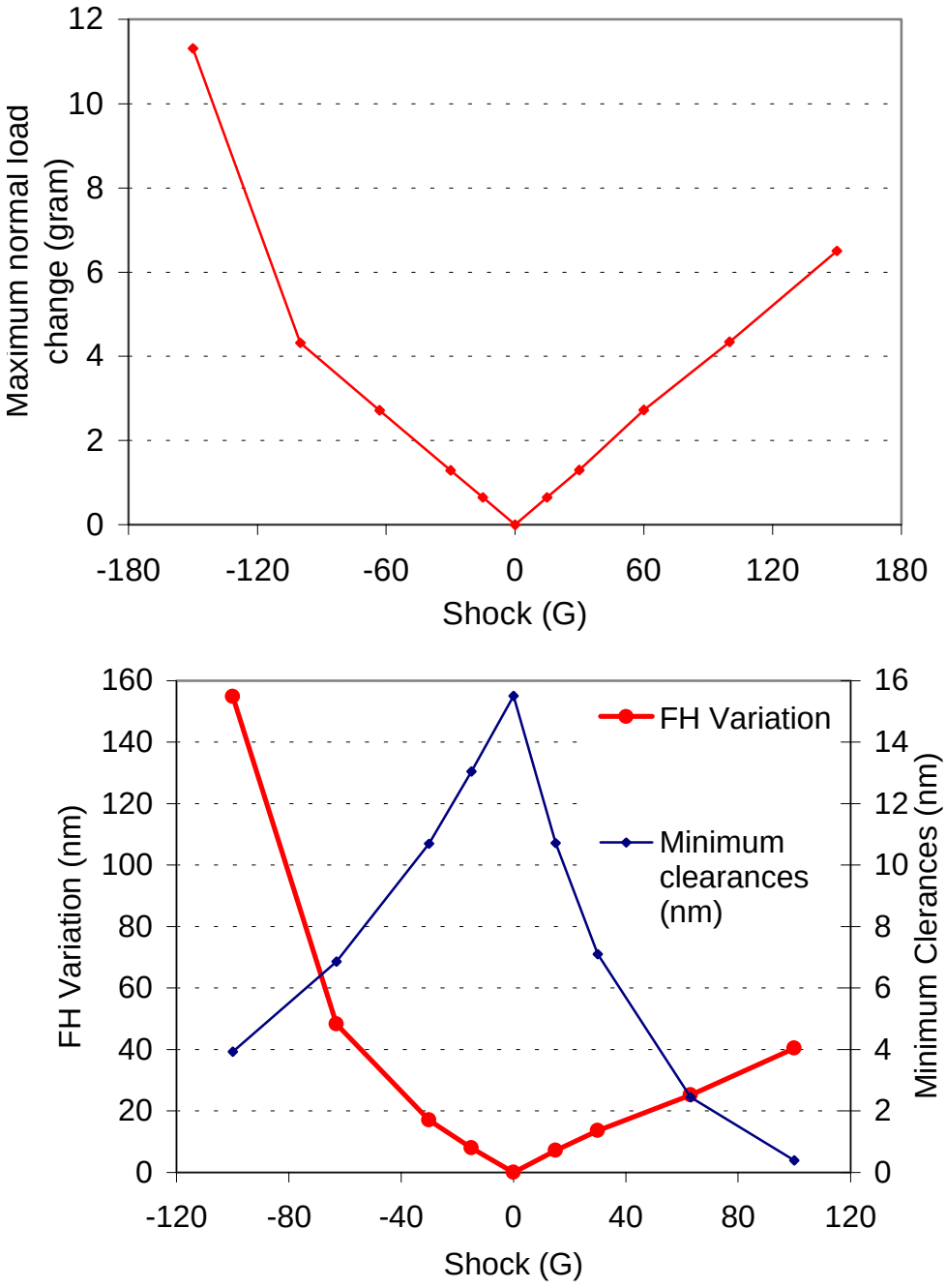

Fig. 14 Comparison of different shock amplitudes